

Electrical properties from photoinduced charging on Cd-doped (100) surfaces of CuInSe₂ epitaxial thin films

Nicole Johnson, Pinar Aydogan, Sefik Suzer, and Angus Rockett

Citation: *Journal of Vacuum Science & Technology A* **34**, 031201 (2016); doi: 10.1116/1.4945105

View online: <https://doi.org/10.1116/1.4945105>

View Table of Contents: <http://avs.scitation.org/toc/jva/34/3>

Published by the [American Vacuum Society](#)

Articles you may be interested in

[RBS-channeling study of radiation damage in Ar⁺ implanted CuInSe₂ crystals](#)

Journal of Vacuum Science & Technology A: Vacuum, Surfaces, and Films **34**, 051203 (2016); 10.1116/1.4961882

[Plasma enhanced atomic layer deposition of zinc sulfide thin films](#)

Journal of Vacuum Science & Technology A: Vacuum, Surfaces, and Films **35**, 01B111 (2017); 10.1116/1.4967724

[Characterization of vacancy defects in Cu\(In,Ga\)Se₂ by positron annihilation spectroscopy](#)

AIP Advances **6**, 125031 (2016); 10.1063/1.4972251

[Doping mechanism in pure CuInSe₂](#)


Journal of Applied Physics **119**, 173103 (2016); 10.1063/1.4947585

[Structural and compositional analyses of Cu\(In,Ga\)Se₂ thin film solar cells with different cell performances](#)

Journal of Vacuum Science & Technology B, Nanotechnology and Microelectronics: Materials, Processing, Measurement, and Phenomena **34**, 03H121 (2016); 10.1116/1.4943518

[Effect of the cadmium chloride treatment on RF sputtered Cd_{0.6}Zn_{0.4}Te films for application in multijunction solar cells](#)

Journal of Vacuum Science & Technology A: Vacuum, Surfaces, and Films **34**, 051202 (2016); 10.1116/1.4960979



Instruments for Advanced Science

Contact Hiden Analytical for further details:
www.HidenAnalytical.com
info@hiden.co.uk

CLICK TO VIEW our product catalogue

Gas Analysis	Surface Science	Plasma Diagnostics	Vacuum Analysis
 <ul style="list-style-type: none">dynamic measurement of reaction gas streamscatalysis and thermal analysismolecular beam studiesdissolved species probesfermentation, environmental and ecological studies	 <ul style="list-style-type: none">UHV TPDSIMSend point detection in ion beam etchelemental imaging - surface mapping	 <ul style="list-style-type: none">plasma source characterizationetch and deposition process reaction kinetic studiesanalysis of neutral and radical species	 <ul style="list-style-type: none">partial pressure measurement and control of process gasesreactive sputter process controlvacuum diagnosticsvacuum coating process monitoring

Electrical properties from photoinduced charging on Cd-doped (100) surfaces of CuInSe₂ epitaxial thin films

Nicole Johnson^{a)}

Department of Materials Science and Engineering, University of Illinois at Urbana-Champaign,
1304 W Green St., Urbana, Illinois 61801

Pinar Aydogan and Sefik Suzer

Department of Chemistry, Bilkent University, 06800 Ankara, Turkey

Angus Rockett

Department of Materials Science and Engineering, University of Illinois at Urbana-Champaign,
1304 W Green St., Urbana, Illinois 61801

(Received 11 January 2016; accepted 18 March 2016; published 5 April 2016)

The photoresponse of Cd-doped CuInSe₂ (CIS) epitaxial thin films on GaAs(100) was studied using x-ray photoelectron spectroscopy under illumination from a 532 nm laser between sample temperatures of 28–260 °C. The initial, air-exposed surface shows little to no photoresponse in the photoelectron binding energies, the Auger electron kinetic energies or peak shapes. Heating between 50 and 130 °C in the analysis chamber results in enhanced n-type doping at the surface and an increased light-induced binding energy shift, the magnitude of which persists when the samples are cooled to room temperature from 130 °C but which disappears when cooling from 260 °C. Extra negative charge trapped on the Cu and Se atoms indicates deep trap states that dissociate after cooling from 260 °C. Analysis of the Cd modified Auger parameter under illumination gives experimental verification of electron charging on Cd atoms thought to be shallow donors in CIS. The electron charging under illumination disappears at 130 °C but occurs again when the sample is cooled to room temperature. © 2016 American Vacuum Society.

[<http://dx.doi.org/10.1116/1.4945105>]

I. INTRODUCTION

Cu(In,Ga)Se₂ (CIGS) is a promising material for the absorber layer in photovoltaic devices due to its modest production cost and chemical flexibility, with champion devices recorded at over 22% efficiency.¹ Many costs associated with producing and distributing photovoltaic modules are related to device area rather than power output. Increasing the device efficiency results in more power per unit area and thus to an overall reduction in levelized cost of electricity. However, CIGS-based photovoltaic devices suffer from a less than optimal open-circuit voltage, which is limited by a variety of defects that promote charge recombination.² Thus, there is potential for further improvements in performance if charge collection and recombination mechanisms can be better understood.

Point defects, thought to be responsible for recombination in CIGS-based devices, have been extensively studied using electrical characterization, including various types of capacitance and admittance spectroscopies.^{3–5} The defects identified as most likely to be a problem are Cu-Se divacancy complexes ($V_{Cu}-V_{Se}$), Se vacancies, and In on Cu (In_{Cu}) antisite complexes with Cu vacancies, the latter of which may contribute to band tails. Nonetheless, there is debate over which defect complex is most critical.^{6–12} Techniques for analyzing these defects in a chemically specific fashion are rare and sometimes unreliable.

Open-circuit voltage, and by extension defects driving recombination, can be investigated by analyzing the surface photovoltage (SPV), which has been directly related to open-circuit voltage in photovoltaics.^{13–15} A simple model for the surface photovoltage suggests that the dipole due to band bending at a semiconductor surface will typically sweep photogenerated minority carriers to the surface, causing the bands to flatten from the resulting charge.¹⁶ Surface defects in Cd-doped CuInSe₂ (CIS) surfaces, such as In dangling bonds and Cd on Cu antisites (Cd_{Cu}) pin the Fermi level close enough to the conduction band to cause downward band bending at the CdS/CIS interface.^{17,18}

It is becoming increasingly important to analyze defect and photovoltage behavior under realistic operating conditions. Methods that can accomplish this are known as *operando* techniques. Examples of methods using photons as the probing particle include some implementations of infrared vibrational spectroscopy, Raman spectroscopy, sum-frequency generation, x-ray emission and absorption spectroscopies, as well as their derivatives. Techniques such as Auger electron spectroscopy and x-ray photoelectron spectroscopy (XPS) have been underutilized due to the high vacuum requirement of the instruments. However, XPS is quite unique in its ability to analyze changes in electron density around individual types of atoms in a solid. The experiment in this study utilizes an *operando* adaptation to XPS using two photon sources, soft x-rays and a 532 nm visible laser. The x-rays produce the measured photoelectron peaks while the visible photons are used to induce the surface charge. Photoelectrons generated by the x-rays in the XPS technique escape from the charge

^{a)}Electronic mail: nejhsn2@illinois.edu

dipole layer near the surface, including traversing any potential due to band bending resulting from the electric field at the surface. This alters their kinetic energy and thus their apparent binding energy (BE) to the atoms from which they were released. The altered kinetic energy appears as a *shift* in the core level binding energies of the characteristic peaks under illumination. Previous work with optically and electrically modulated XPS has included work on relatively well known materials such as Si, GaN and CdS.^{19–21} Additionally a previous study by Hunger *et al.* looked at bare, clean polycrystalline CIS surfaces and found that the surface exhibited a negligible surface charging, which Hunger *et al.* attributed to dangling In bonds that are passivated by S during CdS deposition.¹⁸ Our study complements the existing literature by combining sample heating and illumination to provide new insights into device properties and reliability.

In this work, we combine illumination intensity and temperature to measure changes in surface charging behavior of single crystal films of CIS grown epitaxially on GaAs. Epitaxial films were studied in order to investigate surface charging properties in the absence of grain boundary effects, which are thought to have lateral band bending due to defects along the boundaries.^{22–24} Additionally, surface potential is orientation-dependent, and so it is important to be able to select the surface orientation. Finally, it is important to have relatively flat films to allow the probe depth to be well defined to simplify data interpretation.

This study finds that heating under UHV can reduce or eliminate surface recombination from ambient air contamination and enhance n-type doping in the surface region, leading to the development of a persistent negative surface photovoltage. Further, this study finds a higher surface recombination velocity around the In atoms that correlates with excess negative charge trapped on nearby Se and Cu atoms. Additional analysis of the modified Auger parameter also gives direct experimental evidence of electron charging on Cd donors in CuInSe₂ thin films. Thus, the results help to understand charging and discharging behavior at the CIS surface.

II. EXPERIMENT

CIS films were grown epitaxially on (100)-oriented GaAs substrates. The 500–1000 nm thick films were grown at ~650–700 °C using a hybrid sputtering and evaporation method.²⁵ In this method, Cu and In were cosputtered using separate dc magnetron sources while Se was evaporated from an effusion cell in a single stage process. The targets were located ~30 cm from the substrate. Typically, the sputtering conditions for the two sources were 210 and 350 mA at 330 and 650 V for the Cu and In magnetrons, respectively, at an Ar sputtering gas pressure of 0.28 Pa. The base pressure of the deposition system is $\sim 3 \times 10^{-4}$ Pa. The Se evaporator was ramped to a temperature of 520 °C initially to accelerate heat up and then allowed to cool to the operating condition of 300 °C. The substrates were affixed to a sealed resistively heated holder using spring clips. Substrate temperatures were measured by a thermocouple embedded in the heater

and calibrated using an optical pyrometer. The substrate, magnetrons, and the Se evaporator were covered using shutters until growth was initiated. The substrate was heated at 40 °C/min to the growth temperature and growth was initiated shortly after that temperature was stabilized. After growth, the Se heater and magnetrons were shut off, and the substrate was cooled using a controlled ramp down to 250 °C (720–450 °C in 20 min, 450–350 °C in 20 min, and 350–250 °C in 15 min). The sample heater was then turned off, and the sample was allowed to cool to room temperature. Cu-poor films (Cu:In~0.8) were grown, as this composition is comparable to that used in commercial devices. Films with Cu-poor composition should have a variety of point defects that might trap charge and contribute to surface band bending.^{12,26,27} Typical film compositions before depositing the CdS were 21 at. % Cu, 27 at. % In, and 51 at. % Se as measured by energy dispersive spectroscopy (EDS) with an error of 0.5% based on references to standard films with known composition. X-ray diffraction confirmed the films were phase pure and epitaxial on the GaAs substrates.

Some of the best performing devices utilize a postgrowth treatment under a Se flux.²⁸ The films used in this study had been left out in ambient air after several months and then reintroduced to the deposition chamber for a postgrowth anneal. The anneal occurred under a Se flux at a sample temperature of 450 °C for 15 min. After the heat treatment, the sample was cooled to 250 °C over 20 min, and then, the heater was turned off. Once the sample cooled to room temperature, it was removed and then coated with CdS. The CdS protects the CIS surface from oxidation.

The CdS was deposited via a chemical bath deposition process.^{17,29} Deionized water of 146 ml was heated to ~75 °C. Solutions of 0.015 M CdSO₄ and 1.5 M thiourea were prepared by mixing hydrates of CdSO₄ and thiourea, respectively, with deionized water. CdSO₄ solution of 20 ml, 25 ml of stock 14.8 M NH₄OH, and 10 ml of the thiourea solutions were measured out separately. Samples to be coated were held by clips and blown dry with nitrogen gas to remove any dust particles that had settled on the surface. Once the reaction beaker reached 69 °C, the samples were lowered into the beaker and stirring was turned on to thoroughly mix the contents of the beaker during deposition. The CdSO₄ and the NH₄OH were added first to the reaction beaker, lowering the reaction solution temperature to ~60 °C. The solution was allowed to mix for 1 min before the thiourea was added. The 1 min mixing time allows the NH₄OH to strip any native oxides from the CIS, ensuring a clean reaction surface and so that the CdSO₄ is thoroughly distributed. After adding thiourea, the solution was heated to 65 °C, which was stable over the course of the deposition. The samples were held in the solution for 3 min, taken out, washed with deionized water, and blown dry with nitrogen gas. The reaction beaker solution had turned slightly yellow but was still transparent when the samples were removed. Prior to loading into the XPS chamber, the CdS was etched off using a dilute (~5%) HCl solution, rinsed with deionized water, and blown dry with dry nitrogen. The samples were etched for approximately 2 min. Previous work has shown

that the CIS films are resistant to this etch even after etch times of 18 h.¹⁷ The samples were loaded into the analysis system as rapidly as possible after the etch/rinse/dry steps.

A Kratos Axis Ultra spectrometer was used to measure the photoinduced surface charging of the films. Monochromatic Al K_{α} x-rays with an energy of 1486.8 eV were generated at a source power of 210 W. The samples could be heated during analysis up to 260 °C using a radiant heater, as monitored by a thermocouple on the sample stage. Each temperature was held for 30 min after the ramp to ensure an even temperature on the sample surface. Survey spectra were used to monitor the film composition while high resolution spectra were taken of the Cu $2p_{3/2}$, In $3d_{5/2}$, In 4d, Se 3d, Cd $3d_{5/2}$, Cd 4d peaks and the valence band to determine their positions and shape changes under illumination and temperature changes. Peak positions were calibrated to the Au $4f_{7/2}$ line at 84.00 eV.

To measure the photoresponse of the peak positions, a 532 nm continuous wave laser with a rated power of 50 mW illuminated the sample through one of the system's quartz viewports. The spot size was approximately 2 mm and centered so that it encompassed an area larger than the spectrometer's analysis region (which was $\sim 400 \times 700 \mu\text{m}$ in this work). The photon flux on the sample was calculated to be approximately 1×10^{18} [photons $\text{cm}^{-2} \text{s}^{-1}$]. While the system has a low energy electron flood gun for charge neutralization, it was not used in order to isolate the effect of the laser on the surface electronic properties. The samples were conductive enough to not experience peak drift due to photoelectrons escaping the surface at the x-ray source power used.

III. RESULTS AND DISCUSSION

A. Initial surface chemistry

Survey spectra were obtained at a variety of sample temperatures (28, 50, 80, 100, 130, 180, 230, and 260 °C) to understand changes in composition versus temperature (Fig. 1). The initially loaded surface showed small but measurable amounts of oxygen (~ 12 – 14 at. %) and carbon contamination on the surface. Carbon was not included in the composition analysis because of overlap with one of the Se LMM Auger lines. In addition to the expected CIS film peaks, Cd peaks were observed, and accounted for ~ 8 (at. %) of the analysis volume. No Cl peaks were present, suggesting the water rinse removed any Cl potentially leftover from the HCl etch. The binding energy of the observed Cd $3d_{5/2}$ peak, 405.2 eV, corresponds to a CdSe chemical environment.³⁰ Thus, there should be little to no S present on the surface, suggesting that the HCl etch had selectively removed the CdS. This observation along with the absence of any S peaks in the survey spectrum implies that the Cd was not primarily present as an oxide or sulfide and had been incorporated into the CIS surface rather than adsorbed on the surface, in agreement with previous studies.¹⁷

Quantification of the surface composition over the various temperatures studied was done by correcting peak intensities using relative sensitivity factors specific to the Kratos system. The relative sensitivity factors take into account the mean free path of the photoelectrons, the transmission

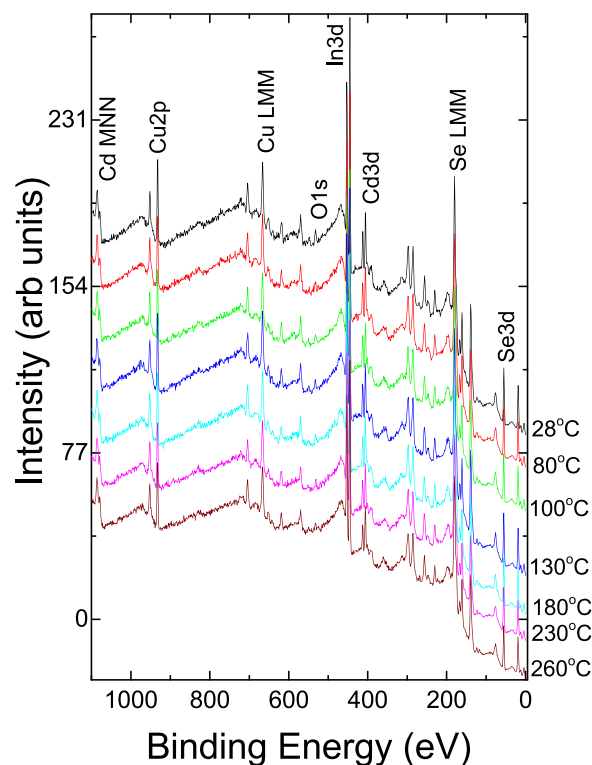


Fig. 1. (Color online) Survey spectra at various sample stage temperatures. Twenty eight degree Celsius is at the top (black) with increasing temperatures downward in the series, ending at 260 °C (brown). The elements indicated (except the O1s) are regions studied in high resolution.

function of the spectrometer and the relative x-ray cross-section. The Shirley background was used for the Cu $2p$, In $3d$, Se $3p$, and Cd $3d$ regions. The film's initial composition at the surface was found to be cation and specifically In rich. Based on the inelastic background and the small O1s peak present in Fig. 1, we conclude that the surface was relatively clean. The average composition was Cu:In:Se:Cd 13:33:46:8 at. %, after elimination of the O contribution, consistent with prior work on clean CIS surfaces.^{22,23} EDS measurements of films in this work have a bulk Cu:In ratio of ~ 0.8 as compared with the surface value of ~ 0.4 measured by XPS, indicating that the surface is indeed Cu deficient. As the sample stage in the analysis chamber was heated, the O concentration declined to below noise levels. We attribute this to O desorption, either as O_2 or residual H_2O contamination, as the CIS film peaks increased in intensity without changing relative to each other.

Initial calibrated Cu $2p_{3/2}$, In $3d_{5/2}$, Se $3d_{5/2}$, and Cd $3d_{5/2}$ emission energies were measured as 932.0, 444.6, 54.2, and 405.2 eV, respectively. Linear regression from the leading edge of the valence band can be used to determine the position of the valence band maximum.³¹ In this work, the valence band maximum was 0.6 eV from the Fermi level. The bulk of the films are p-type, so we attribute the increased difference between the Fermi level and the valence band as due to donor type surface states such as In dangling bonds or Cd doping that shift the Fermi level to just above midgap. The binding energy values for the In $3d_{5/2}$ and Se $3d_{5/2}$ peaks are consistent with CuInSe_2 , and the Cd $3d_{5/2}$ peak binding

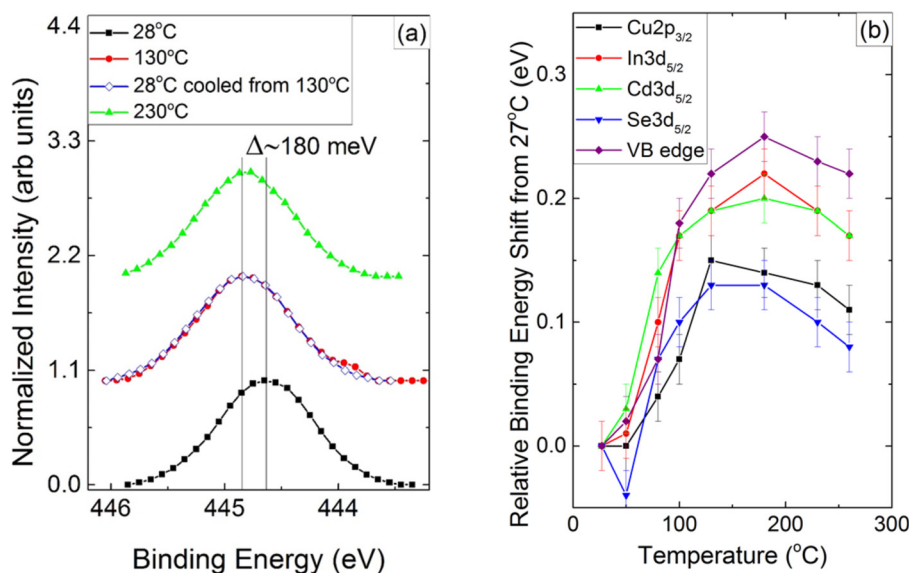


FIG. 2. (Color online) (a) In_{3d_{5/2}} normalized intensity vs binding energy in the dark at 28 °C (black squares), 130 °C (red circles), 28 °C cooled from 130 °C (blue empty diamonds), and 230 °C (green triangles). (b) Binding energy shift in the dark vs temperature for all core level peaks and the valence band edge between 28 and 260 °C relative to room temperature value.

energy was consistent with a CdSe chemical environment within the error of the spectrometer.³⁰ The Cu 2p_{3/2} peak is slightly higher in binding energy than expected, although not so high that it can be attributed to Cu₂Se.³² A better indicator of the chemical environment is the modified Auger parameter defined as the $\alpha' = BE_p + KE_A$, where p represents the core level and A represents the Auger line.³³ Auger parameters were calculated for the Cu (BE Cu 2p_{3/2} + KE Cu LMM Auger line), Cd (BE Cd 3d_{5/2} + KE Cd MNN Auger line) and Se (BE Se 3d_{5/2} + KE Se LMM Auger line) atoms as 1849.3, 787.2, and 1361.4 eV, respectively. The Cu and Se Auger parameters are consistent with Cu-poor films of CuInSe₂.³⁴ The Cd Auger parameter turned out to be too big to be CdSe, but we believe positive charge trapping on the Cd atoms may be affecting the Auger parameter as discussed in Sec. III B.

B. Heating in the dark: 28–260 °C

The core level spectra were obtained at the same temperatures indicated in the survey scans. Upon heating in the analysis chamber without illumination, the peak binding energies for all elements and the valence band edge shift toward higher binding energies (Fig. 2). This behavior has been reported in the literature for polycrystalline CIS surfaces and has been attributed to increased n-type doping at the surface, which, in turn, enhances the surface band bending.^{22,23} However, in that case, the authors measured the peak shifts after cooling to room temperature while in this work we measured the peak positions while the sample was held at temperature. The peaks all shift together toward higher binding energies until 100 °C was reached, indicating an increase in n-type surface doping likely from activation of Cd donor defects or electron release from other shallow donors.

This work also differs from the literature in that not all peaks shifted by the same amount under heating. After 100 °C,

the Cu2p and Se3d peaks start to deviate from the rest of the core levels and valence band. If one assumes that all the peaks shift together when the surface doping is enhanced, then the Cu and Se atoms seem to be surrounded by extra negative charge that offsets the band bending. When cooling to room temperature from 130 °C, the binding energies of all peaks remain the same as at 130 °C, indicating the surface doping, and thus the band bending, remain constant after cooling.

We interpret these observations as follows. Net negative charge is being transferred from the In and Cd to the Cu and Se atoms. We anticipate that In on Cu sites (In_{Cu}) and Cd on Cu sites (Cd_{Cu}) act as donors, consistent with the observed In-rich, Cd-doped surface composition, and transfer the negative charge to Cu and Se atoms at the surface. This is also consistent with the slightly Se-deficient surface composition that would be promoted by net negative charge on the Se sites. The additional positive charge on the In atoms causes the In core levels to shift to higher binding energy. However, this is accompanied by a shift in the Fermi energy as the surface is more n-type. Thus we propose that the shift in the In core levels is matched by a shift in the valence band associated with the In_{Cu} n-type doping of the surface, such that there is no shift in the In core levels *relative* to the Fermi energy. The negative charge on the Cu and Se atoms appears to be discharged after cooling to room temperature from 260 °C as all the Se core level peaks show the same amount of shift compared to their as-loaded values.

Beyond 180 °C, the surface starts to become less n-type. This is seen in Fig. 2(b) as all of the core level peaks and valence band edge shift approximately together toward lower binding energies. The extra negative charge on the Cu and Se atoms is still present even at these temperatures. One mechanism for this behavior could be Cd diffusion, which is thought to occur via Cu vacancy substitution. While bulk Cd diffusion was not observed in epitaxial films until

$\sim 400^\circ\text{C}$,³⁵ the extremely Cu-poor surface could provide enough Cu vacancies for Cd diffusion to occur near the CIS surface. We did not see a decrease in the Cd atomic concentration within the error of the spectrometer. However, above 180°C , the intensity of the $\text{Cd}3d_{5/2}$ peak relative to the $\text{In}3d_{5/2}$ peak started to decrease substantially. Therefore, there could be evidence of Cd surface diffusion at temperatures as low as 180°C .

To further investigate the chemical state of the elements within our samples, we calculated the modified Auger parameters for the Cu, Cd, and Se atoms at sample temperatures of 28°C (initial load), 80, 130, and 28°C after cooling from 130°C (Fig. 3). The Auger parameters for Cu and Se are consistent within $\pm 0.1\text{ eV}$ of what has been reported for CuInSe_2 . The Cd Auger parameter in our work is significantly higher ($>0.1\text{ eV}$) than reported for the CdSe, the CdO, and the $\text{Cd}(\text{OH})_2$ chemical environments. From previous work, we expect that the Cd is sitting on Cu sites, meaning it should make bonds to four selenium atoms (close to CdSe chemical environment). However, Cd in the surface of CIS on Cu sites has second-nearest neighbor cations very different from CdSe. Thus, it is very likely that there would be charge on the Cd atoms, changing its overall charge state. Such charging would affect the modified Auger parameter and gives information about whether a species is oxidized or reduced, which has been used to study oxidation of the CIS

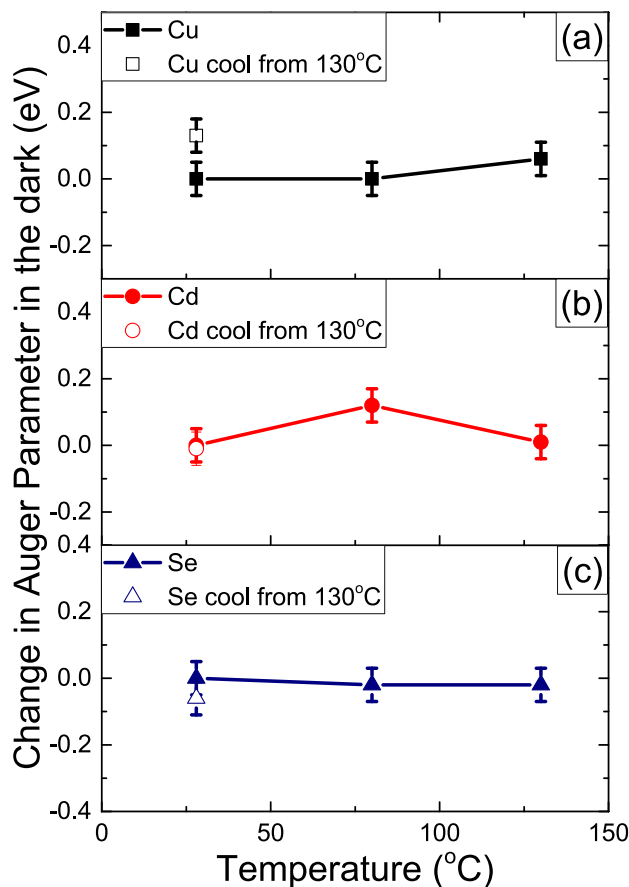


Fig. 3. (Color online) Modified Auger parameters compared to room temperature values for (a) Cu, (b) Cd and (c) Se at sample temperatures 28°C (initial load), 80, 130, and 28°C after cooled from 130°C .

surface under air exposure.³⁶ We looked at a similar analysis of the modified Auger parameter, but in this case under heat for the dark and illuminated cases instead of air exposure. A higher than expected Auger parameter indicates a reduction of the Cd atoms, making them more positively charged than expected for the CdSe environment. As the sample is heated, there is a negligible effect on the Cu, Cd, and Se modified Auger parameters within the error of measurement. This indicates there is no chemical or charge change purely as a result of temperature. However, illumination does seem to affect the modified Auger parameter as seen in Sec. III C.

C. Photoresponse under illumination

Illuminating the initial air exposed surface showed little effect on the peak position or shape (Fig. 4). The small photoresponse at room temperature was observed over a range of x-ray source powers from 10 to 210 W. We propose that the negligible photoresponse is due to high surface recombination rates resulting from defect states that limit the accumulation of photogenerated carriers. This behavior appears to be related to air exposure since samples heated to 130°C maintained a large photoresponse after cooling to 28°C under UHV but reverted to a small photoresponse after re-exposure to air. The higher photoresponse can be

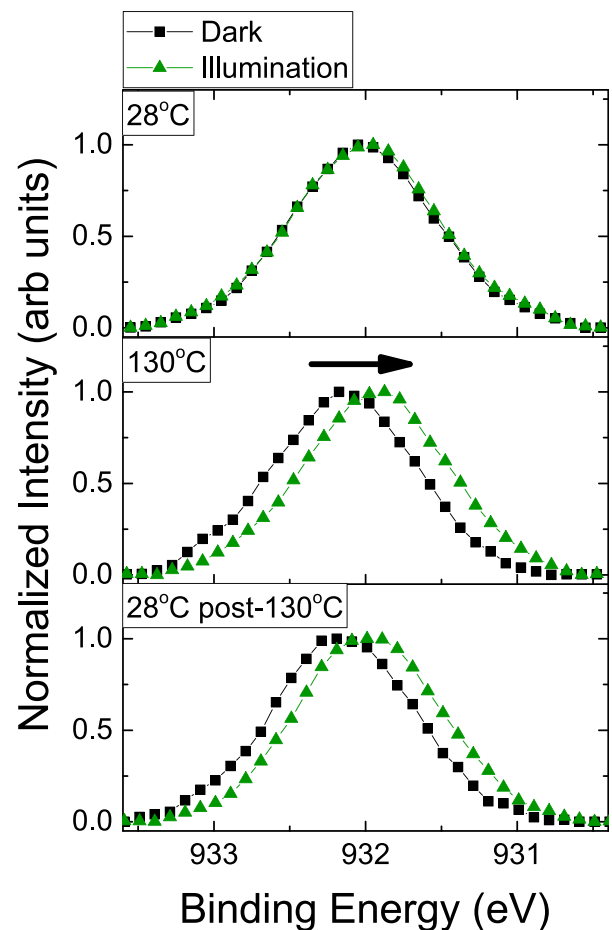


Fig. 4. (Color online) $\text{Cu}2p_{3/2}$ peak in the dark and under illumination at 28°C (initial loading), 130°C and cooled to 28°C from 130°C . Under illumination, the peak shifts toward lower binding energies (see arrow).

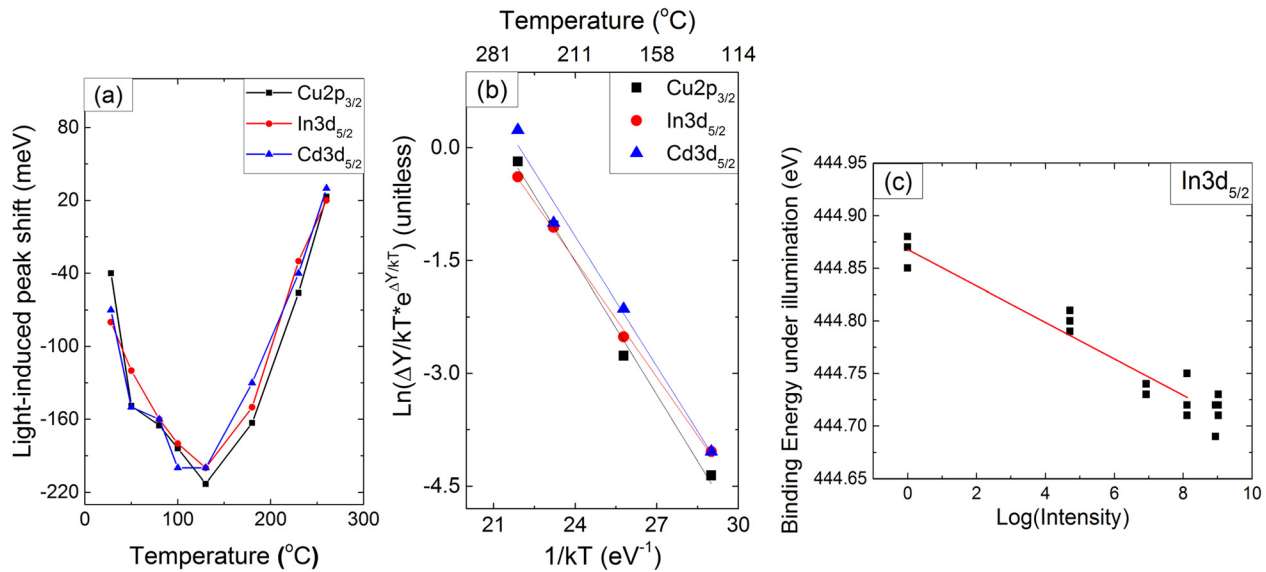


FIG. 5. (Color online) (a) Laser-induced peak shift (ΔY) in meV vs the sample temperature for the In3d_{5/2} and the Cu2p_{3/2} peaks, (b) laser-induced peak shift vs temperature (130–260 °C) with the lines indicating the line of best fit to the data using a linear fit following the formalism of Eq. (2), and (c) In3d_{5/2} BE vs the log of the laser intensity at sample temperature 130 °C.

recovered again by heating the sample under UHV to 130 °C. Thus, there appears to be a need for an O free CIS/CdS interface, which agrees with observations showing that oxygen at the junction resulted in poorer device performance.²³

The air-induced states observed here are unlikely to result from simple surface oxides as no additional components were observed in the CIS or Cd core level peaks that would indicate the presence of Cu, In, Se, or Cd oxides for the air-exposed films. Furthermore, the expected oxides would not likely desorb with gentle heating. We note that between room temperature and 130 °C, there is a decrease in O concentration that correlates with an increase in the light-induced peak shift.

Binding energy changes due to illumination are a function of temperature and illumination as seen in Fig. 5. Once the sample has been heated to as little as 50 °C, illumination caused a shift, consistent in both value and direction, in the binding energy of all core level peaks and the valence band edge toward lower binding energies. This suggests the presence of a surface photovoltage. The value of this shift saturates at $\sim -(150\text{--}200)$ meV for a sample temperature of 130 °C as seen in Fig. 5(a) for the Cu2p_{3/2} and In3d_{5/2} peaks. Changing the intensity using neutral density filters results in a logarithmic dependence of the photoinduced shift versus the light intensity [Fig. 5(c)], confirming the surface photovoltage nature of the photoresponse.¹⁶

Quantitative information on the surface recombination velocity can be obtained by combining the intensity and temperature dependence of the surface photovoltage response. Assuming a thermionic model, which has been used to study surface charging properties in n-type GaN,³⁷ the steady-state SPV can be fit with the following equation:

$$\Delta Y = \eta kT \text{Ln} \left(1 + \frac{cP_o}{R_o} \right), \quad (1)$$

where ΔY is the light-induced shift, η is the ideality factor, k is Boltzmann's constant, T is the temperature, c represents the fraction of photons absorbed in the depletion region, P_o is the photon flux, and R_o is the rate that carriers move from the bulk to the surface under dark conditions. Fitting the data using best fit values of 0.5 for c and 1.1 for η gave values for R_o of 2.5, 3, and $4 \times 10^{15} \text{ cm}^{-2} \text{ s}^{-1}$ based on data for the In 3d_{5/2}, Cd 3d_{5/2}, and Cu 2p_{3/2} photoelectrons, respectively. From the same model as in Ref. 33, R_o can be used to find the surface recombination velocity if the band bending is known. The temperature dependence of the photoresponse gives that information using the following equation by Tanaka *et al.*:¹⁶

$$\text{Ln} \left(\frac{\Delta Y}{kT} e^{(\Delta Y/kT)} \right) = \text{Ln}(I) + \frac{Y_o}{kT}, \quad (2)$$

where I is the laser intensity and Y_o is the band bending in the dark. Figure 5(b) plots the left hand side of the equation versus $1/kT$. When plotted, the slope of this curve is the band bending, which was measured as -0.52 ± 0.01 eV, -0.58 ± 0.05 eV, and -0.59 ± 0.03 eV for the In 3d_{5/2} and the Cd 3d_{5/2} and Cu 2p_{3/2} photoelectrons, respectively. The error was found based on the least squares method.

Surface recombination velocity can now be solved for using

$$S_n = e^{(-Y_o + (E_c - E_f)/kT)} \frac{R_o}{N_c}, \quad (3)$$

where N_c is the density of states at the conduction band minimum and $E_c - E_f$ is the difference between the conduction band edge and the Fermi level. Without accounting for a possibly higher bandgap at the surface (due to missing Cu), values for the surface recombination velocity were an order of magnitude lower than those reported previously for clean CuInSe₂ surfaces (10^4 vs $10^5 \text{ cm}^{-1} \text{ s}^{-1}$).³⁸ Because the chemical bath deposition process has resulted in higher efficiency devices, it is

possible that this process is responsible for the improved surface recombination of the CIS even when the CdS is subsequently removed. This could help explain the relative success of Cd partial-electrolyte treatments. Alternatively, heating under UHV could have inhibited surface recombination since the surface recombination velocity was measured after the films had been cooled from 130 °C.

What is interesting here is that the surface recombination velocities were element dependent. The surface recombination velocity measured using the In 3d photoelectrons was $(2 \pm 0.7) \times 10^4 \text{ cm s}^{-1}$ was approximately an order of magnitude higher than the velocity measured using the Cu or Cd photoelectrons, which was measured at $(2.06 \pm 2.39) \times 10^3 \text{ cm s}^{-1}$ and $(2.28 \pm 4.40) \times 10^3 \text{ cm s}^{-1}$, respectively. The errors are large enough that the Cu and Cd electrons have effectively the same surface recombination velocity but are distinct from the surface recombination velocity measured using the In photoelectrons. When considering the potential defects, the evidence from the valence band and core level shifts in the dark suggests that the In and Cd atoms are relatively positively charged compared to the negative Cu and Se atoms. However, the surface recombination velocities imply that the In atoms have a higher trapping rate for electrons than the Cd, despite both being donors at relatively equivalent probe depths in the XPS technique. The In_{Cu} donor has a +2 charge state when fully ionized so when an electron becomes trapped, the defect is still repulsive to holes since it now exists in a +1 charge state. This suggests that the rate-limiting step in recombination is probably capture of holes rather than electrons on the In. It makes sense that the recombination velocity is higher since the +2 charge state makes it more attractive to electrons traveling toward the surface. In comparison, the Cd_{Cu} donor has a +1 charge state when fully ionized. When an electron is trapped on this donor, the defect is neutral and holes could recombine with the trapped electrons relatively easily. Thus, recombination on donors with a charge state of +1 or lower is likely limited by electron capture, opposite to defects with a charge state of +2 or higher.

Charge trapping behavior becomes more apparent when looking at the differences in the modified Auger parameter under illumination (Fig. 6) where zero represents no change under illumination. The Cu and Se Auger parameters show no significant deviation ($<0.1 \text{ eV}$) under light and increasing temperature compared to their initial values at room temperature. However, under illumination, there is a significant increase in the Cd modified Auger parameter at 28 and 80 °C. This increase disappears at 130 °C. An increase in the modified Auger parameter indicates an oxidation process, making the Cd more negatively charged. This electron trapping is consistent with Cd being a donor in CIS. At 130 °C, the electron charging disappears presumably due to thermal escape of electrons from the Cd atoms. This suggests that the energy level associated with this Cd point defect is between 30 and 34 meV because the change in Auger parameter under illumination goes to zero somewhere between 80 and 130 °C, consistent with a shallow donor.

When the sample was cooled to 28 from 130 °C, the Cd modified Auger parameter still increases under illumination,

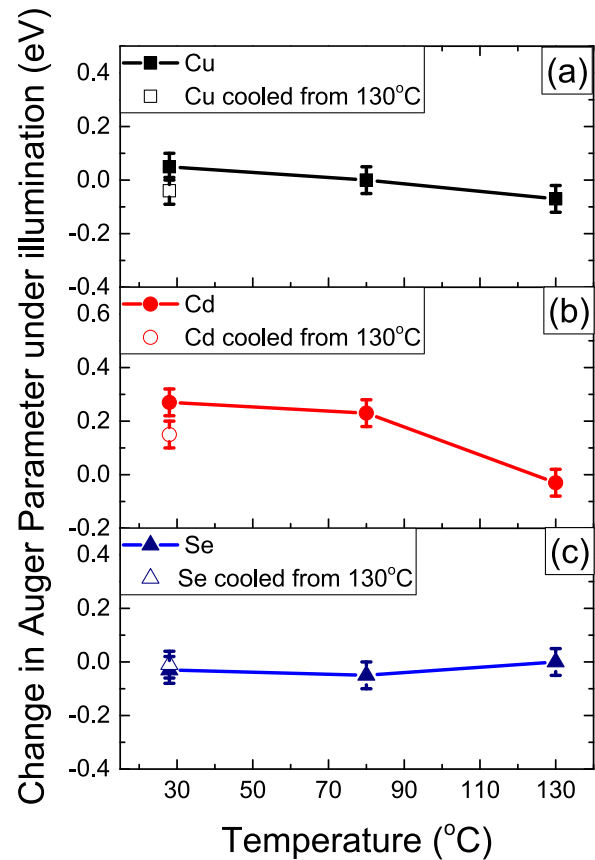


Fig. 6. (Color online) Modified Auger parameters under illumination compared to values in the dark for (a) Cu, (b) Cd, and (c) Se at sample temperatures 28 °C (initial load), 80 °C, 130 °C, and 28 °C after cooled from 130 °C.

but not as much as it did before cooling. This suggests that electron trapping on Cd atoms under illumination is due to changes in the Cd donor charge state. Because there is no change in the Se modified Auger parameter, we conclude that the electron charging is localized on the Cd atoms only.

Additionally, the band bending can be used to determine bulk material properties. As mentioned above, the band bending was measured at $\sim -0.59 \text{ eV}$ for the Cu photoelectrons. $E_f - E_v$ between 130 and 260 °C was approximately constant at -0.69 eV . Because the Cu 2p photoelectrons should be the most surface sensitive and show the maximum band bending at the surface, this value is used to construct the diagram of the sample surface (Fig. 7). In the analysis used to construct (Fig. 7), we use 13.6 for the dielectric constant (ϵ), 1.02 eV for the bulk bandgap, and calculate $1.5 \times 10^{19} \text{ cm}^{-3}$ and $6.7 \times 10^{17} \text{ cm}^{-3}$ for N_v and N_c , respectively, from effective masses reported in Rockett and Birkmire,³⁹ which gives an intrinsic carrier concentration of $9 \times 10^9 \text{ cm}^{-3}$. Knowing these values, we can use the following to calculate the depletion region (W)⁴⁰

$$W = \sqrt{\frac{2\epsilon(Y_o - kT)}{qN_A}}. \quad (4)$$

From those values, the depletion region is calculated to be approximately $0.44 \mu\text{m}$.

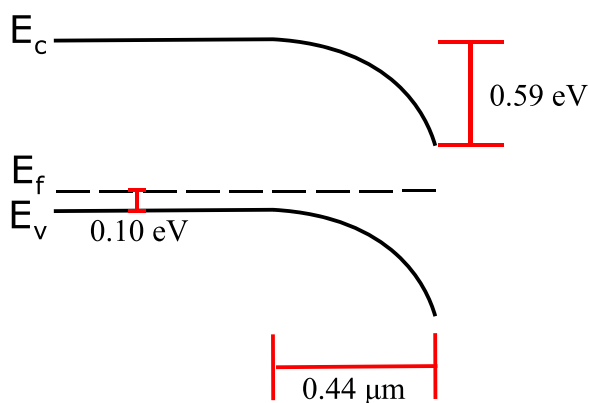


FIG. 7. (Color online) Schematic of the band edge energy vs distance from the sample surface at sample temperatures 130–260 °C. Knowing $E_f - E_v$ and the band bending allows for calculation of bulk doping and depletion width.

IV. SUMMARY AND CONCLUSIONS

We have demonstrated that this *operando* XPS technique can observe changes in surface electronic properties due to changes in surface doping, charging of shallow donor states created by Cd atoms, and surface recombination velocity in a chemically specific way. High recombination surface states due to air exposure can be passivated via heating at low temperatures. Enhanced n-type doping is maximized at 130 °C, which gives the highest photoresponse of $-(150\text{--}200)$ meV. Heating in the dark shows excess negative charge on/near the Cu and Se atoms, which we believe is caused by charge trapping. Whatever is responsible for this behavior disappears after cooling the sample to room temperature from 260 °C. The temperature and intensity dependence of the photoresponse allowed us to measure the band bending and surface recombination behavior in a chemically specific fashion, which suggests that surface recombination occurs preferably on the In atoms compared to the Cu and Cd atoms. This could indicate a higher defect density around the In atoms, possibly from defects or defect complexes involving some of the In atoms. Detailed analysis of the modified Auger parameter suggests electron charging localized on Cd atoms between room temperature and 130 °C, confirming the Cd atoms' shallow donor behavior. Finally, the photoresponse appears to abruptly decrease after cooling to room temperature from 230 to 260 °C, which suggests Cd diffusion when compared to the decrease in the peak intensity of the Cd photoelectron peak compared to the other film constituents.

ACKNOWLEDGMENTS

The authors would like to thank their funding agencies and research facilities. This work was partially supported by the National Science Foundation (NSF) through the Grant No. DMR-1312539 and the Turkish Scientific and Technological Research Council of Turkey (TUBITAK) through the Grant No. 212 M051. XPS, EDS, and XRD were carried out in part in the Frederick Seitz Materials Research Laboratory Central

Research Facilities, University of Illinois. A special thanks to Rick Haasch at the UIUC for helping collect the XPS spectra.

- ¹Solar Frontier, "Solar Frontier Achieves World Record Thin-Film Solar Cell Efficiency: 22.3%," (2015), available at <http://www.solar-frontier.com/eng/news/2015/C051171.html>.
- ²A. L. Fahrenbruch and R. H. Bube, *Fundamentals of Solar Cells: Photovoltaic Solar Energy Conversion* (Academic, New York, 1983).
- ³T. Walter, R. Herberholz, C. Müller, and H. W. Schock, *J. Appl. Phys.* **80**, 4411 (1996).
- ⁴J. Lucas, C. Longeaud, T. Bertram, and S. Siebentritt, *Appl. Phys. Lett.* **104**, 153905 (2014).
- ⁵M. Igalson and H. W. Schock, *J. Appl. Phys.* **80**, 5765 (1996).
- ⁶D. Huang and C. Persson, *J. Phys. Condens. Matter* **24**, 455503 (2012).
- ⁷C. Stephan, S. Schorr, M. Tovar, and H.-W. Schock, *Appl. Phys. Lett.* **98**, 091906 (2011).
- ⁸J. Pohl and K. Albe, *Phys. Rev. B* **87**, 245203 (2013).
- ⁹E. Korhonen, K. Kuitunen, F. Tuomisto, A. Urbaniak, M. Igalson, J. Larsen, L. Gütay, S. Siebentritt, and Y. Tamm, *Phys. Rev. B* **86**, 064102 (2012).
- ¹⁰S. Lany and A. Zunger, *J. Appl. Phys.* **100**, 113725 (2006).
- ¹¹S. Niki *et al.*, *Thin Solid Films* **387**, 129 (2001).
- ¹²L. E. Oikkonen, M. G. Ganchenkova, A. P. Seitsonen, and R. M. Nieminen, *J. Phys. Condens. Matter* **23**, 422202 (2011).
- ¹³Y. Fu, T. Rada, C.-H. Fischer, M. C. Lux-Steiner, and T. Dittrich, *Prog. Photovolt. Res. Appl.* **22**, 44 (2014).
- ¹⁴Y.-J. Lee, J. Wang, and J. W. P. Hsu, *Appl. Phys. Lett.* **103**, 173302 (2013).
- ¹⁵B. Goldstein, *Appl. Phys. Lett.* **39**, 258 (1981).
- ¹⁶S. Tanaka, S. D. More, J. Murakami, M. Itoh, Y. Fujii, and M. Kamada, *Phys. Rev. B* **64**, 155308 (2001).
- ¹⁷D. Liao and A. Rockett, *J. Appl. Phys.* **93**, 9380 (2003).
- ¹⁸R. Hunger, M. V. Lebedev, K. Sakurai, T. Schulmeyer, T. Mayer, A. Klein, S. Niki, and W. Jaegermann, *Thin Solid Films* **515**, 6112 (2007).
- ¹⁹U. K. Demirok, G. Ertas, and S. Suzer, *J. Phys. Chem. B* **108**, 5179 (2004).
- ²⁰H. Sezen, A. A. Rockett, and S. Suzer, *Anal. Chem.* **84**, 2990 (2012).
- ²¹H. Sezen, E. Ozbay, and S. Suzer, *Appl. Surf. Sci.* **323**, 25 (2014).
- ²²S. Bröker, D. Kück, A. Timmer, I. Lauer mann, B. Ümsür, D. Greiner, C. A. Kaufmann, and H. Mönig, *ACS Appl. Mater. Interfaces* **7**, 13062 (2015).
- ²³H. Mönig, D. Lockhorn, N. Aghdassi, A. Timmer, C. A. Kaufmann, R. Caballero, H. Zacharias, and H. Fuchs, *Adv. Mater. Interfaces* **1**, 1300040 (2014).
- ²⁴D. Fuertes Marrón, S. Sadewasser, A. Meeder, T. Glatzel, and M. C. Lux-Steiner, *Phys. Rev. B* **71**, 033306 (2005).
- ²⁵A. Rockett, T. C. Lommasson, P. Campos, L. C. Yang, and H. Talieh, *Thin Solid Films* **171**, 109 (1989).
- ²⁶S. B. Zhang, S.-H. Wei, A. Zunger, and H. Katayama-Yoshida, *Phys. Rev. B* **57**, 9642 (1998).
- ²⁷L. E. Oikkonen, M. G. Ganchenkova, A. P. Seitsonen, and R. M. Nieminen, *J. Phys. Condens. Matter* **26**, 345501 (2014).
- ²⁸F. S. Hasoon, Y. Yan, H. Althani, K. M. Jones, H. R. Moutinho, J. Alleman, M. M. Al-Jassim, and R. Noufi, *Thin Solid Films* **387**, 1 (2001).
- ²⁹J. Kessler, K. O. Velthaus, M. Ruckh, R. Laichinger, and H. W. Schock, *Proceedings of the 6th International Photovoltaic Science and Engineering Conference*, New Delhi, India (1992), p. 1005.
- ³⁰M. Polak, *J. Electron Spectrosc. Relat. Phenom.* **28**, 171 (1982).
- ³¹T. Gleim *et al.*, *Surf. Sci.* **531**, 77 (2003).
- ³²L. L. Kazmerski, *J. Vac. Sci. Technol.* **19**, 467 (1981).
- ³³C. D. Wagner, L. H. Gale, and R. H. Raymond, *Anal. Chem.* **51**, 466 (1979).
- ³⁴E. Niemi and L. Stolt, *Surf. Interface Anal.* **15**, 422 (1990).
- ³⁵A. Aquino and A. Rockett, *J. Vac. Sci. Technol.* **31**, 021202 (2013).
- ³⁶D. Hauschild, F. Meyer, S. Pohlner, R. Lechner, R. Dietmüller, J. Palm, C. Heske, L. Weinhardt, and F. Reinert, *J. Appl. Phys.* **115**, 183707 (2014).
- ³⁷J. D. McNamara, M. Foussekis, H. Liu, H. Morkoc, M. A. Reshchikov, and A. A. Baski, *Proc. SPIE* **8262**, 826213 (2012).
- ³⁸S. Mora and N. Romeo, *J. Appl. Phys.* **48**, 4826 (1977).
- ³⁹A. Rockett and R. W. Birkmire, *J. Appl. Phys.* **70**, R81 (1991).
- ⁴⁰S. M. Sze and K. K. Ng, *Physics of Semiconductor Devices*, 3rd ed. (Wiley-Interscience, Hoboken, NJ, 2007).